Available online at www.sciencedirect.com
ScienceDirect
Polymer 47 (2006) 6738–6744
polymer
www.elsevier.com/locate/polymer

Preparation, characterization and antimicrobial activity of chitosan/layered silicate nanocomposites

Xiaoying Wang, Yumin Du*, Jianhong Yang, Xiaohui Wang, Xiaowen Shi, Ying Hu

Department of Environmental Science, College of Resource and Environmental Science, Wuhan University, Wuhan, Hubei 430079, PR China

Received 20 February 2006; received in revised form 16 May 2006; accepted 15 July 2006
Available online 7 August 2006

Abstract

Chitosan/layered silicate nanocomposites with different ratios were successfully prepared via solution-mixing processing technique. Unmodified Ca^{2+}-rectorite and organic rectorite modified by cetyltrimethyl ammonium bromide were used. Their structures were characterized by XRD, TEM and FT-IR techniques. The results showed that chitosan chains were inserted into silicate layers to form the intercalated nanocomposites. The interlayer distance of the layered silicates in the nanocomposites enlarged as its amount increased. When the weight ratio between chitosan and organic rectorite was 12:1, the largest interlayer distance of 8.24 nm was obtained. However, with further increase of its amount, the interlayer distance of the layered silicates in the nanocomposites reduced. In vitro antimicrobial assay showed that pristine rectorite could not inhibit the growth of bacteria, but chitosan/layered silicate nanocomposites had stronger antimicrobial activity than pure chitosan, particularly against Gram-positive bacteria. With the increase of the amount and the interlayer distance of the layered silicates in the nanocomposites, the nanocomposites showed a stronger antibacterial effect on Gram-positive bacteria, while the nanocomposites showed a weaker antibacterial effect on Gram-negative bacteria. The lowest minimum inhibition concentration (MIC) value of the nanocomposites against *Staphylococcus aureus* and *Bacillus subtilis* was 0.00313% (w/v), and the relative inhibition time (RIT) against *B. subtilis* with concentration of 0.00313% (w/v) was >120 h.

Keywords: Chitosan; Rectorite; Nanocomposite

1. Introduction

In recent years, polymer/layered silicate nanocomposites have attracted considerable interest since they combine the structure, physical and chemical properties of both inorganic and organic materials. Most work with polymer/layered silicate nanocomposites has concentrated on montmorillonite (MMT) [1] although rectorite (REC) may be more preferred. REC is another kind of layered silicate with structure and characteristic much like those of montmorillonite. It is a sort of regularly interstratified clay mineral with alternate pairs of dioctahedral mica-like layer (nonexpansible) and dioctahedral montmorillonite-like layer (expansible) in a 1:1 ratio. The separable layer thickness and layer aspect ratio (area–thickness) of REC are larger than those of regular montmorillonite [2]. These characteristics may be favorable for forming the intercalated or exfoliated nanocomposites, and help to improve the efficiency of reinforcement of nanolayers in many properties.

Although several types of polymer/layered silicate nanocomposite products with different shapes and applications including food packaging films and containers, engine parts, dental materials, etc. are now available in markets [3], polymer/layered silicate nanocomposites with antimicrobial activity, which will be very much favorable to the nanocomposites' applications are rarely seen.

Chitosan (CS) is a high molecular weight polysaccharide composed of β-(1,4)-2-acetamido-2-deoxy-D-glucose and β-(1,4)-2-amino-2-deoxy-D-glucose units. As a natural antimicrobial agent, the antibacterial and antifungal activities of CS have been widely reported, suggesting high killing rate, broad

* Corresponding author. Tel./fax: +86 27 68778501.
E-mail address: duyumin@whu.edu.cn (Y. Du).

0032-3861/$ - see front matter © 2006 Elsevier Ltd. All rights reserved.
doi:10.1016/j.polymer.2006.07.026

spectrum of activity and low toxicity towards mammalian cell [4]. In order to improve its antimicrobial activity further, some researchers have prepared complexes of CS with certain materials, which also exhibited good bacteriostatic activity such as surfactants [5], metals [6], essential oils [7] and some organic acids [8]. On the other hand, it should be noted that modified layered silicates could adsorb both natural and anthropogenic toxin [9,10] and exhibit an inhibitory property for the proliferation of bacteria. So it is a good opportunity to prepare the CS/layered silicate nanocomposites that will exhibit enhanced antimicrobial activity. Until recently, there are only a limited number of reports about chitosan/layered silicate nanocomposites based on MMT [11–13]. Darder et al. synthesized functional CS/MMT nanocomposites, which have been successfully used in the development of bulk modified electrodes [11,12]. Wang et al. reported the effect of acetic acid residue and MMT loading in the nanocomposites [13]. They prepared the CS/MMT nanocomposites based only on pristine MMT rather than modified MMT, so the obtained interlayer distance was not very large, which may affect directly the great improvement of the material properties. In other cases, CS/layered silicate nanocomposites dealing with REC have scarcely been reported, which will be proved as a good intercalation effect in our work.

In the present work, organic rectorite (OREC) was first prepared by means of cation exchange. Then a series of CS/layered silicate nanocomposites were synthesized. Their structures were characterized by XRD, TEM and FT-IR techniques. Thermal stability was confirmed by TG analysis. Antibacterial activity of the nanocomposites was evaluated.

2. Experimental

2.1. Materials

Chitosan (CS) from a shrimp shell was purchased from Yuhuan Ocean Biochemical Co. (Taizhou, China). The degree of deacetylation was 92% (determined by elemental analysis) [14] and its weight average molecular weight was 2.1×10^5 (determined by GPC method) [15].

Calcium rectorite (Ca^{2+}-REC) refined from the clay minerals was provided by Hubei Mingliu Inc. Co. (Wuhan, China). Cetyltrimethyl ammonium bromide (CTAB) was supplied by Xinrui Science and Technology Inc. Co. (Wuhan, China). All other chemicals were of analytical grade.

2.2. Synthesis of organic rectorite

The organic rectorite (OREC) was prepared by a cation exchange between Ca^{2+}-rectorite galleries and CTAB in an aqueous solution. Rectorite (4 g) was dispersed in distilled water to obtain clay suspension using a stirrer, and left standing for 24 h after vigorous stirring for 30 min. CTAB (2 g) was dissolved in water, and then dropped slowly into the REC suspension at 90 °C under stirring. After stirring for 5 h, the product was washed several times with distilled water and filtered to ensure the complete removal of bromide ions, which were detected with $AgNO_3$ until no AgBr precipitate was found. The product was dried at 90 °C to yield OREC.

2.3. Preparation of the chitosan/layered silicate nanocomposites

CS was dissolved in 1% (w/v) acetic acid to prepare the 0.5% (w/v) solution. The resulting solution was added slowly into the pretreated OREC and REC suspensions under stirring at 60 °C to obtain nanocomposites with initial CS/OREC weight ratios of 2:1, 6:1, 12:1, 20:1, and 50:1 and CS/REC ratios of 6:1, 12:1, and 20:1. The resulting mixture was agitated for 2 days, and then precipitated with 1 mol/l NaOH. The formed composites were washed with distilled water until the solution became neutral. Finally the nanocomposites were dried at 50 °C and ground to powder.

2.4. Characterizations of nanocomposites

The X-ray diffraction (XRD) experiment was performed using a diffractometer type D/max-rA (Tokyo, Japan) with Cu target and Kα radiation ($\lambda = 0.154$ nm) at 40 kV and 50 mA. The scanning rate was 0.02°/min and the scanning scope of 2θ was 0.7–10° and 5–45° at room temperature.

Ultrathin films for transmission electron microscopy (TEM) were prepared by cutting from the epoxy block with the embedded nanocomposite sheet at room temperature using an LKB-8800 ultratome. The TEM micrographs were taken using a transmittance electron microscope [JEM-2010 FEF (UHR), JEOL, Japan] at an accelerating voltage of 200 kV.

IR spectra were recorded in KBr pellets on a Nicolet FT-IR 5700 spectrophotometer (Madison, USA) by the method of transmission.

Thermogravimetry (TG) was performed using a Setaram Setsys 16 TG/DTA/DSC (France) under a nitrogen atmosphere of 0.15 MPa from 25 to 600 °C and at a heating rate of 10 °C/min.

2.5. Antibacterial assays

Gram-positive bacteria *Staphylococcus aureus*, *Bacillus subtilis* and Gram-negative bacteria *Escherichia coli, Pseudomonas aeruginosa* were provided by China Center for Type Culture Collection (CCTCC at Wuhan University) and incubated on nutrient agar (peptone 1%, beef extract 0.5%, NaCl 0.5%, agar 2%, pH = 7.2).

The antibacterial activity of the nanocomposites was evaluated by finding the minimum inhibition concentration (MIC) and the relative inhibition time (RIT) as follows: the microorganism suspension was adjusted by sterile distilled water to 10^5–10^6 cell/ml. The nanocomposites, CS, REC and OREC solutions were prepared in acetate buffer (pH = 5.4) at a concentration of 1% (w/v). The resulting solutions and the nutrient agar were autoclaved at 121 °C for 20 min. The twofold serial dilutions (1 ml) of each sample were added to sterile petri-dishes together with 9 ml nutrient agar to the final concentrations of 0.1% (w/v), 0.05% (w/v), 0.025% (w/v), 0.0125% (w/v),

0.00625% (w/v), 0.00313% (w/v), and 0.00156% (w/v). A loop of each microorganism suspension was inoculated on cooled nutrient medium by means of drawing a stripe. The bacteria were cultured at 37 °C. MIC values were read after a 24 h culture and RITs were obtained after 5 days.

The minimum inhibition concentration (MIC) was defined as the lowest concentration required to inhibit the growth of the bacteria, i.e. the concentration at which no microorganism colony or less than 5 colonies were visible within 19–38 h. Relative inhibition time (RIT) was determined by the time when the bacterial colonies were deterred to grow, i.e. the difference between the time when colonies in the experiments were visible on agar plates and the corresponding time in the control plates [5].

3. Results and discussion

3.1. Structure and morphology

Fig. 1(A) shows XRD patterns of Ca^{2+}-rectorite and OREC. Ca^{2+}-rectorite exhibits $2\theta = 3.59°$ and the Δd_L value (the interlayer distance) is 2.45 nm, calculated by the Bragg's equation. In comparison with REC, the d_{001} peak of OREC shifts towards lower angle ($2\theta = 3.16°$) and the Δd_L value is 2.94 nm. This fact confirms that CTAB has been intercalated into the interlayer of unmodified Ca^{2+}-rectorite [2]. XRD curves for the nanocomposites prepared from CS with different unmodified REC and OREC contents are presented in Fig. 1(B) and (C). The characteristic 001 diffraction peaks of all the nanocomposites shift towards low angles as compared to the pristine REC, it reveals that the CS chains have inserted into the layered silicates and the intercalated nanocomposites with a larger Δd_L values have formed. Interestingly, the interlayer distance of all the nanocomposites is not proportional to the amount of untreated REC and OREC, indicating that the Δd_L values are not affected by the amount of the layered silicates, which is in accordance with the previous report [16]. The interlayer distance of the layered silicates enlarged as its amount increased. When the mass ratio between chitosan and organic rectorite was 12:1, the largest interlayer distance of 8.24 nm was obtained. But with further increase of its amount, the interlayer distance of the layered silicates reduced. And it can be found that the intercalation effect of CS/OREC nanocomposites was much better than that of CS/REC nanocomposites. The fact may be because the modified agent has greatly improved the hydrophobic nature and allowed the CS to interact better with the layered silicates [17]. Besides, in comparison with the CS/MMT nanocomposites [11–13], CS/layered silicate nanocomposites based on REC have shown better intercalation effect, which will be favorable for greatly improving the material properties.

TEM micrographs of CS/clay nanocomposites are shown in Fig. 2 in two levels of magnification. The dark lines and the bright area represent the clay and the CS matrix, respectively. Distinguishable clay particles show the extent of clay particle dispersion in the polymeric matrix [18]. The micrographs clearly indicate that the silicate layers are dispersed well

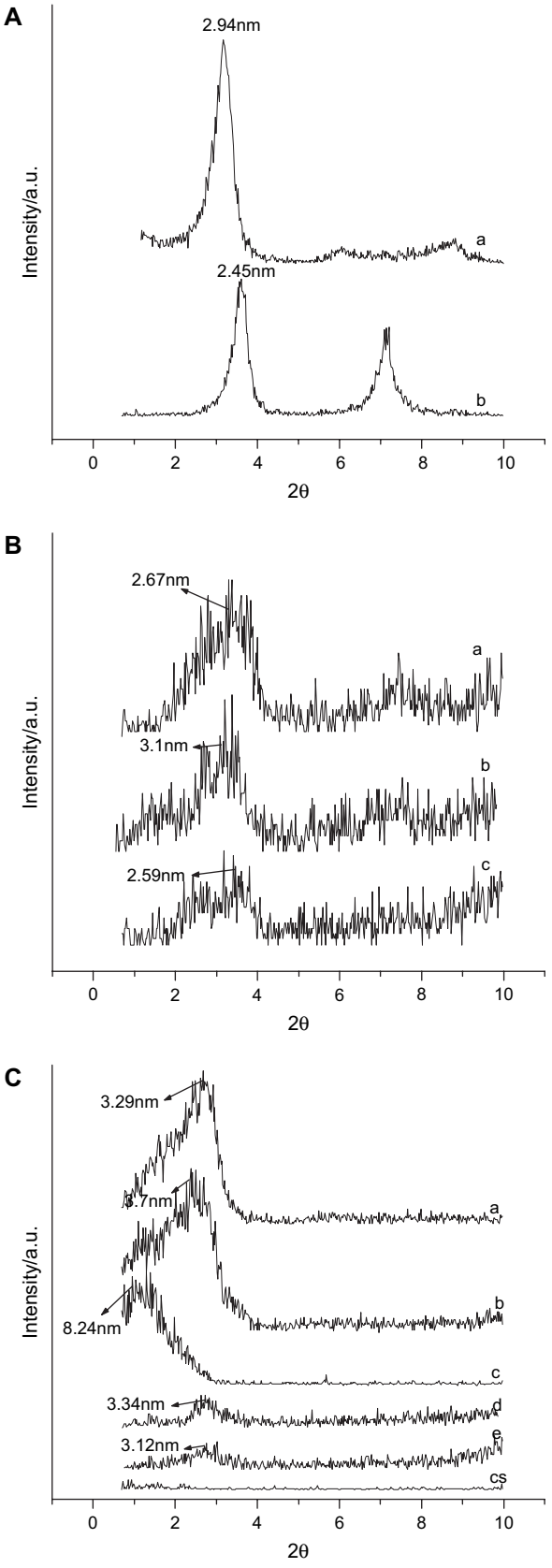

Fig. 1. (A) XRD patterns of (a) OREC and (b) unmodified REC. (B) XRD pattern of nanocomposites with different CS/REC ratios of (a) 6:1, (b) 12:1, and (c) 20:1. (C) XRD patterns of CS and nanocomposites with different CS/OREC ratios of (a) 2:1, (b) 6:1, (c) 12:1, (d) 20:1, and (e) 50:1.

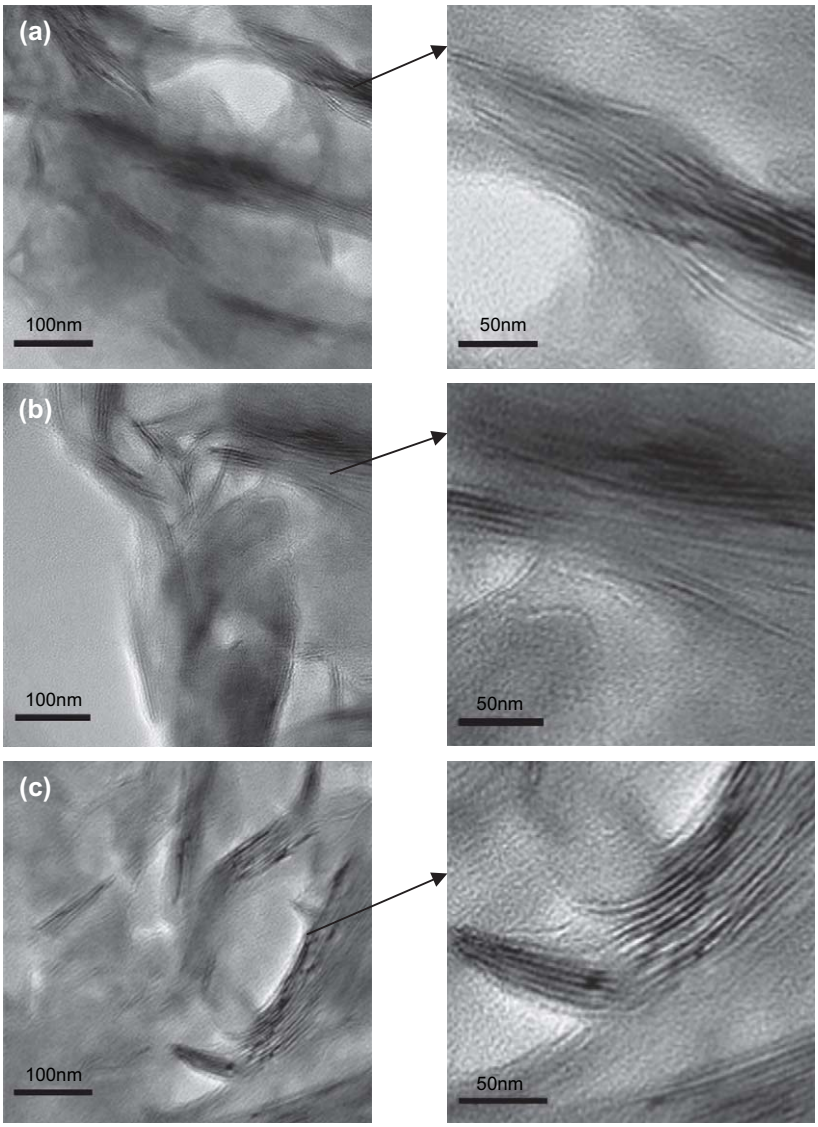

Fig. 2. TEM micrographs of nanocomposites with different CS/OREC ratios of (a) 6:1, (b) 12:1, and (c) with CS/REC ratio of 12:1.

into the CS matrix at a nanometer scale. Moreover, few aggregated clay can be observed in the 6:1 CS/clay nanocomposites as compared to the 12:1 CS/clay nanocomposites, that is to say, as the content of clay increased, most of the layered silicates can disperse uniformly in these CS/layered silicate nanocomposites. Good dispersion of clay in the polymer matrix will have a significant effect on the properties of the nanocomposites. A closer observation of the micrograph reveals that most of the layers (especially in picture a and picture c) are stacked together, this is because the layers were intercalated rather than exfoliated with the Δd_L value of only around 3 nm (see the XRD results and the micrographs at high magnification in Fig. 2). The presence of those multiplets was also observed by Kornmann et al. in epoxy–clay nanocomposites [19]. Besides, it should be noted that some layers are apart in picture b, as demonstrated by the large Δd_L value of 8.24 nm by the XRD analysis, and it means that few exfoliations occurred for the 12:1 CS/OREC nanocomposite.

As shown in Fig. 3, in comparison with REC, OREC has additional adsorption peaks appearing at 2921 cm^{-1} and 2851 cm^{-1} which belong to $-CH_2-$, $-CH_3$ stretching vibrations; the result reveals again that CTAB has been exchanged into the interlayer of unmodified Ca^{2+}-rectorite [16]. In the spectra of the nanocomposites, the N–H bonded to O–H vibration band at 3448 cm^{-1} in CS shifts towards lower frequency, wider and stronger peaks are observed in all the CS/OREC nanocomposites. This fact indicates that $-NH_2$ and –OH groups of CS formed hydrogen bonds with the –OH group in REC which coincided with the CS/MMT nanocomposites [13]. Another reason may be related to a strong hydrogen bonding interaction between CS molecules and inside CS molecules when constrained into the gallery of REC layers. Evidence for this is seen in the spectra of the 12:1 CS/OREC nanocomposite with the largest loading of CS chains into the interlayer of REC, where the N–H and O–H vibrations shift to the lowest frequency (3419 cm^{-1}) of all

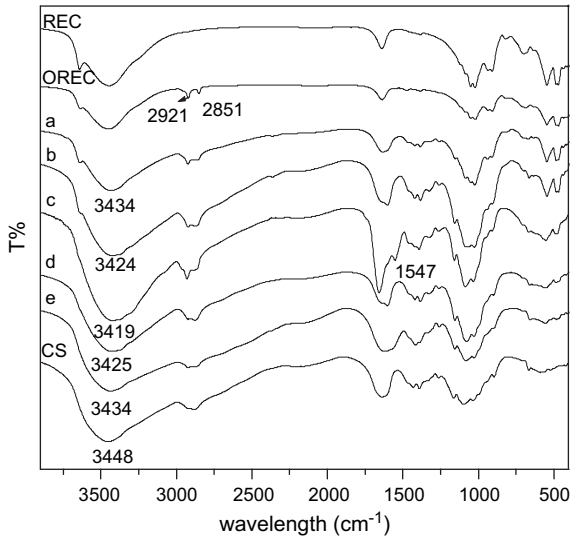

Fig. 3. FT-IR spectra of REC, OREC, CS and nanocomposites with different CS/OREC ratios of (a) 2:1, (b) 6:1, (c) 12:1, (d) 20:1, and (e) 50:1.

the nanocomposites. In addition, a new peak at 1547 cm^{-1} appears in the spectra of this 12:1 CS/OREC nanocomposite, it can be further concluded that the interaction between CS and REC has happened.

As suggested in Fig. 4, the crystal peak near 10° in the nanocomposites gradually disappears and the crystal peak near 20° becomes wider and weaker as compared to pure CS. It is evident that the addition of REC greatly changed the crystallinity of CS. This fact confirms the strong interaction between CS and REC as well.

Based on the above analysis, it can be established that CS had interacted strongly with clay and was intercalated into the interlayer of clay. In addition, the CS chains were sandwiched between the silicate layers while the well ordered multilayer morphology of clay was still present.

3.2. Thermal analysis

TG curves of CS and the nanocomposites are shown in Fig. 5. Obviously, these curves of the nanocomposites are similar to those of CS, in which the two-temperature stages of maximum weight-loss rate can be observed [20]. It can be seen that T_{max} (the temperature when the rate of weight loss reaches a maximum) of the nanocomposites is higher than that of CS, while their weight loss is less than that of CS, it means that the nanocomposites exhibited better thermal stability than did the pure chitosan. It can be resulted from the interaction between CS and clay. Because REC nanolayers with high aspect ratio acted as barriers, they may strongly hinder the volatility of the decomposed products obtained from pyrolysis and limit the continuous decomposition of CS [16]. Furthermore, when CS chains were in a restrained state in the gallery space of the layered structure, CS maintained the fractional free volume smaller [21]; besides hydrogen bonding both between CS molecules and between CS and clay was promoted (see the FT-IR analysis), so the reduced mobility of CS chains may be another important factor to induce an enhancement of thermal stability of the nanocomposites.

It can be further observed that the 2:1 CS/OREC nanocomposite with the highest amount of OREC has the highest T_{max}, while the 12:1 CS/OREC nanocomposite with the largest interlayer distance has a T_{max} similar to the 6:1 CS/OREC nanocomposite. It implies that the thermal properties are directly proportional to the interlayer distance and the amount of clay. With the increase of the amount of clay as barriers, the barrier behavior was further enhanced as a result of good dispersion. Similarly, as the interlayer distance enlarged, more CS chains between the interlayer formed hydrogen bond, and more fractional free volume became small, then the mobility of more CS chains was reduced. Accordingly, the good thermal stability was obtained. Therefore, conclusion

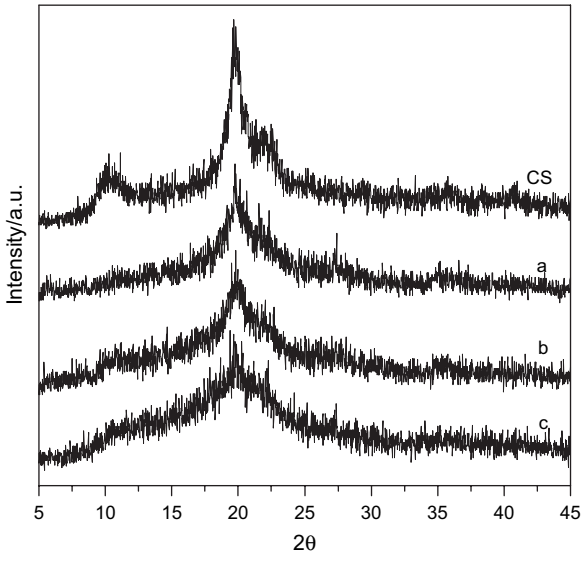

Fig. 4. XRD patterns of CS and nanocomposites with different CS/OREC ratios of (a) 6:1, (b) 12:1, and (c) 20:1.

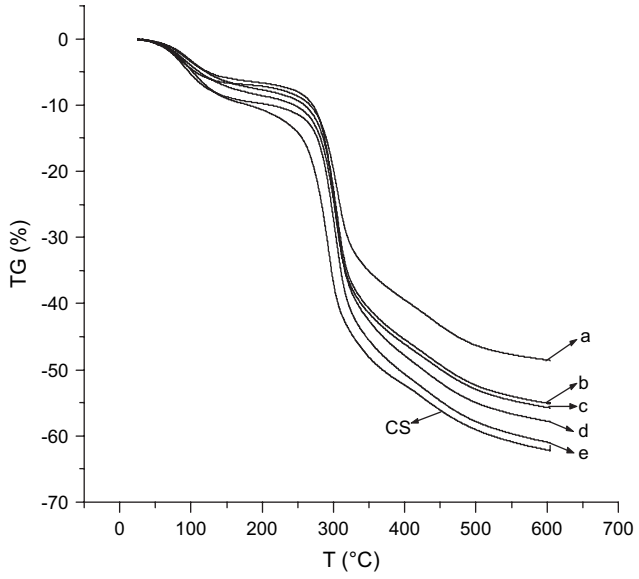

Fig. 5. Thermogravimetry curves of CS and nanocomposites prepared from CS/OREC ratios of (a) 2:1, (b) 6:1, (c) 12:1, (d) 20:1, and (e) 50:1.

can be drawn that the interlayer distance and the amount of clay can result in significant effect on the properties of CS/clay nanocomposites, just like the following antibacterial activity.

3.3. Antimicrobial activity

As to investigate whether REC and OREC themselves have antibacterial properties, REC and OREC were tested when dissolved in acetate buffer. As seen in Table 1, untreated REC has hardly inhibited the bacterial growth, whereas OREC only shows a slight antibacterial activity. And all the nanocomposites show better inhibitory effect than pure CS, REC and OREC.

As shown in Tables 1 and 2, all the nanocomposites show excellent inhibition effect on Gram-positive bacteria. The MIC values of the nanocomposites are 4–30 times lower than that of CS, and the RITs of the nanocomposites are more than 3 times longer than that of CS.

It was suggested that a main factor for the antibacterial activity could be due to the positively charged amino groups at C-2 in the CS molecule in solution below its pK_a (6.3) [22], they could interact with the predominantly anionic molecules at the cell surface. This interaction could change the permeability of the cell membrane of the microorganisms, resulting in a leakage of intercellular components [22], and then caused the death of the cell [23]. On the other hand, it was reported that clay with large specific surface area could adsorb the bacteria from the solution and immobilize the bacteria with the help of its excellent adsorption capacity [9], although the natural clay doesn't have inhibitory effect on bacteria. In this system, the antibacterial process of CS/clay nanocomposites may be divided into two stages. The first stage was the adsorption of the bacteria from the solution and immobilization on the surface of the clay. The second stage was related to the accumulation of CS on the surface of the clay; CS chains were in order and aggregated when confined in the interlayer of the silicates, positive charge (amino groups) density in unit volume may increase, accordingly, the stronger interaction between amino groups and bacteria may occur. Hence, the nanocomposites have better inhibitory effect on the growth of bacteria as compared to pure CS. In addition, it is seen that the CS/OREC nanocomposites show much stronger antibacterial activity than the CS/REC nanocomposites. The result indicates that the cooperation effect of CS, REC and CTAB may induce excellent inhibition properties on the Gram-positive bacteria for the CS/OREC nanocomposites.

In addition, it can be observed that the higher amount and the larger Δd_L value of the layered silicates resulted in the stronger inhibitory activity against Gram-positive bacteria. And the 2:1 CS/OREC nanocomposite with the highest amount of OREC and the 12:1 CS/OREC nanocomposite with the largest interlayer distance show the strongest antibacterial activity. As the amount of clay increased, the effective layers in unit weight may increase because of good dispersion (see TEM results), thereupon larger specific surface area was obtained, and more bacteria were adsorbed and immobilized on the surface of clay, then CS inhibited them. In the same way, with the increase of the interlayer distance, specific surface area of the layers also magnified; besides more CS chains were inserted into the interlayer and positive charge density in unit volume further increased; in this way, CS may have more chance to inhibit the growth of the bacteria. Therefore, alternatively, the increase of the amount or the interlayer distance may result in the improvement of the inhibitory activity against Gram-positive bacteria.

However, the inhibitory activity against Gram-negative bacteria for the nanocomposites is not as good as the inhibitory activity against Gram-positive bacteria. The MIC values of the nanocomposites are only 2–4 times lower than that of CS, and the RITs of nanocomposites are just 2–3 times longer than that of CS. Moreover, as the amount and the interlayer distance of clay increase, the nanocomposites show decreasing inhibitory effect on Gram-negative bacteria. The fact may be related to the cell structure of the bacteria: Gram-positive bacteria have thick cell wall and no outer membrane, whereas Gram-negative bacteria have thin cell wall and its most layers

Table 1
MICs (%) (w/v) of nanocomposites comparing with CS, REC and OREC against different microorganisms

Sample	Gram-positive bacteria		Gram-negative bacteria	
	Staphylococcus aureus	*Bacillus subtilis*	*Escherichia coli*	*Pseudomonas aeruginosa*
Acetate buffer (pH = 5.4)	(0.1)[a]	–	(0.1)	–
CS	0.025	0.1	0.05	0.1
REC	(0.1)	–	(0.1)	–
OREC	0.05	0.05	0.1	0.1
CS/OREC nanocomposites (CS:OREC)				
2:1	0.00313	0.00313	0.025	0.05
6:1	0.00625	0.0125	0.025	0.05
12:1	0.00313	0.00625	0.025	0.05
20:1	0.0125	0.025	0.0125	0.025
50:1	0.0125	0.025	0.0125	0.025
CS/REC nanocomposites (CS:REC)				
2:1	0.025	0.025	0.05	0.1
12:1	0.0125	0.025	0.05	0.1
20:1	0.025	0.05	0.025	0.05

[a] Ineffective at the tested concentration is shown in brackets.

Table 2
RITs (h) of CS and different nanocomposites against different microorganisms

Sample	Concentrations	Gram-positive bacteria		Gram-negative bacteria	
		Staphylococcus aureus	*Bacillus subtilis*	*Escherichia coli*	*Pseudomonas aeruginosa*
Chitosan	0.05	24	<24	24	<12
CS/OREC nanocomposites (CS:OREC)					
2:1	0.05	>120	>120	48	24
6:1	0.05	>120	>120	48	24
12:1	0.05	>120	>120	48	24
20:1	0.05	>120	120	72	48
50:1	0.05	>120	72	72	48
CS/REC nanocomposites (CS:REC)					
6:1	0.05	>120	72	24	12
12:1	0.05	>120	72	24	12
20:1	0.05	120	72	48	24

are outer membranes [5]. Hence, pure CS may have different action mechanisms against Gram-negative bacteria and Gram-positive bacteria [24–26]. Furthermore, the adsorption action of the layered silicates against two species of bacteria may also be different. Further studies should be done to explain the fact.

4. Conclusions

A series of CS/layered silicate nanocomposites were successfully synthesized which indicated a good intercalation of the polymeric phase into clay interlayer galleries. FT-IR and XRD results showed the interaction between CS matrix and REC. It was the interaction that caused the enhanced thermal stability and antimicrobial activity in comparison with pure CS, and they were proportional to the amount and the interlayer distance of the layered silicates. With the increase of the amount and the interlayer distance of the layered silicates, the nanocomposites showed stronger antibacterial effect on Gram-positive bacteria, while the nanocomposites showed weaker antibacterial effect on Gram-negative bacteria. There were several possibilities to explain the results about Gram-positive bacteria, but for Gram-negative bacteria, consideration was only taken from its different cell structure according to the present work. Further work should be done to explain the results.

The results from this study may be used as a foundation for the future development of new types of polymer/layered silicate nanocomposite materials with antimicrobial activity.

References

[1] Giannels EP, Krishnamoorti R, Manias E. Adv Polym Sci 1999;138:107–47.
[2] Ma XY, Lu HJ, Liang GZ, Yan HX. J Appl Polym Sci 2004;93:608–14.
[3] Pinnavaia TJ, Beal GW. Polymer–clay nanocomposites. 1st ed. England: Wiley; 2001 [chapter 5].
[4] Shahidi F, Arachchi JKV, Jeon YJ. Trends Food Sci Technol 1999;10:37–51.
[5] Liu H, Du YM, Yang JH, Zhu HY. Carbohydr Polym 2004;55:291–7.
[6] Wang XH, Du YM, Liu H. Carbohydr Polym 2004;56:21–6.
[7] Zivanovic S, Chi S, Draughon AF. J Food Sci 2005;70:45–51.
[8] Hu SG, Jou CH, Yang MC. Biomaterials 2003;24:2685–93.
[9] Lemke SL, Grant PG, Phillips TD. J Agric Food Chem 1998;46:3789–96.
[10] Guo T, Ma YL, Guo P, Xu ZR. Vet Microbiol 2005;105:113–22.
[11] Darder M, Colilla M, Ruiz-Hitzky E. Chem Mater 2003;15:3380–774.
[12] Darder M, Colilla M, Ruiz-Hitzky E. Appl Clay Sci 2005;28:199–208.
[13] Wang SF, Shen L, Tong YJ, Chen L, Phang IY, Lim PQ, et al. Polym Degrad Stab 2005;90:123–31.
[14] Xu J, McCarthy SP, Gross RA. Macromolecules 1996;29:3436–40.
[15] Qin CQ, Du YM, Xiao L. Polym Degrad Stab 2002;76:211–8.
[16] Li Y, Liu L, Zhang WA, Fang YE. Radiat Phys Chem 2004;69:467–71.
[17] Doh JG, Cho I. Polym Bull 1998;41:511–8.
[18] Pourabas B, Raeesi V. Polymer 2005;46:5533–40.
[19] Kornmann X, Lindberg H, Berglund LA. Polymer 2001;42:1303–10.
[20] Liu YL, Su YH, Lai JY. Polymer 2004;45:6831–7.
[21] Wang ZF, Wang B, Qi N, Zhang HF, Zhang LQ. Polymer 2005;46:719–24.
[22] Papineau AM, Hoover DG, Knorr D, Farkas DF. Food Biotechnol 1991;5:45–57.
[23] Helander IM, Nurmiaho-Lassila EL, Ahvenainen R, Rhoades J, Roller S. Int J Food Microbiol 2001;71:235–44.
[24] Rabea EI, Badawy MET, Stevens CV, Smagghe G, Steurbaut W. Biomacromolecules 2003;4:1457–65.
[25] Huang RH, Du YM, Zheng LS, Liu H, Fan LH. React Funct Polym 2004;59:41–51.
[26] Tokura SK, Ueno S, Miyazaki S, Nishi N. Macromol Symp 1997;120:1–9.